^{68}Ga-DOTATATE PET/CT in the Localization of Head and Neck Paragangliomas Compared with Other Functional Imaging Modalities and CT/MRI

Ingo Janssen[1,2], Clara C. Chen[3], David Taieb[4], Nicholas J. Patronas[5], Corina M. Millo[6], Karen T. Adams[1], Joan Nambuba[1], Peter Herscovitch[6], Samira M. Sadowski[7], Antonio T. Fojo[8], Inga Buchmann[2], Electron Kebebew[7], and Karel Pacak[1]

[1]Program in Adult and Reproductive Endocrinology, Eunice Kennedy Shriver National Institute of Child Health and Human Development, National Institutes of Health, Bethesda, Maryland; [2]Section of Nuclear Medicine, Department of Radiology and Nuclear Medicine, University Hospital Schleswig Holstein, Lübeck, Germany; [3]Nuclear Medicine Division, Radiology & Imaging Sciences, Warren Grant Magnuson Clinical Center, National Institutes of Health, Bethesda, Maryland; [4]Department of Nuclear Medicine, La Timone University Hospital, CERIMED, Aix-Marseille University, Marseille, France; [5]Section of Neuroradiology, Radiology and Imaging Sciences, Warren Grant Magnuson Clinical Center, National Institutes of Health, Bethesda, Maryland; [6]Positron Emission Tomography Department, Warren Grant Magnuson Clinical Center, National Institutes of Health, Bethesda, Maryland; [7]Endocrine Oncology Branch, National Cancer Institute, Bethesda, Maryland; and [8]Center for Cancer Research, National Cancer Institute, Bethesda, Maryland

Pheochromocytomas/paragangliomas overexpress somatostatin receptors, and recent studies have already shown excellent results in the localization of sympathetic succinate dehydrogenase complex, subunit *B*, mutation-related metastatic pheochromocytomas/paragangliomas using ^{68}Ga-DOTATATE PET/CT. Therefore, the goal of our study was to assess the clinical utility of this functional imaging modality in parasympathetic head and neck paragangliomas (HNPGLs) compared with anatomic imaging with CT/MRI and other functional imaging modalities, including ^{18}F-fluorohydroyphenylalanine (^{18}F-FDOPA) PET/CT, currently the gold standard in the functional imaging of HNPGLs. **Methods:** ^{68}Ga-DOTATATE PET/CT was prospectively performed in 20 patients with HNPGLs. All patients also underwent ^{18}F-FDOPA PET/CT, ^{18}F-FDG PET/CT, and CT/MRI, with 18 patients also undergoing ^{18}F-fluorodopamine (^{18}F-FDA) PET/CT. ^{18}F-FDOPA PET/CT and CT/MRI served as the imaging comparators. **Results:** Thirty-eight lesions in 20 patients were detected, with ^{18}F-FDOPA PET/CT identifying 37 of 38 and CT/MRI identifying 23 of 38 lesions ($P < 0.01$). All 38 and an additional 7 lesions ($P = 0.016$) were detected on ^{68}Ga-DOTATATE PET/CT. Significantly fewer lesions were identified by ^{18}F-FDG PET/CT (24/38, $P < 0.01$) and ^{18}F-FDA PET/CT (10/34, $P < 0.01$). **Conclusion:** ^{68}Ga-DOTATATE PET/CT identified more lesions than other imaging modalities. With the results of the present study, and the increasing availability and use of DOTA analogs in the therapy of neuroendocrine tumors, we expect that ^{68}Ga-DOTATATE PET/CT will become the preferred functional imaging modality for HNPGLs in the near future.

Key Words: ^{68}Ga-DOTATATE; ^{18}F-FDOPA; head and neck paraganglioma

J Nucl Med 2016; 57:186–191
DOI: 10.2967/jnumed.115.161018

Received May 18, 2015; revision accepted Sep. 21, 2015.
For correspondence or reprints contact: Karel Pacak, Section on Medical Neuroendocrinology, Eunice Kennedy Shriver NICHD, NIH, Building 10, CRC, Rm. 1E-3140, 10 Center Dr. MSC-1109, Bethesda, MD 20892.
E-mail: karel@mail.nih.gov
Published online Nov. 12, 2015.

Head and neck paragangliomas (HNPGLs) are neuroendocrine tumors (NETs) derived from the parasympathetic nervous system (*1,2*), representing approximately 0.6% of all head and neck tumors (*3*). These tumors mainly occur in the carotid body (CB) (60%), glomus vagale (GV) (13%), glomus jugulare (GJ) (23%), or glomus tympanicum (6%) regions (*4*). Depending on their localization and multiplicity, up to 38% or more of HNPGLs in patients with a negative family history are hereditary (*5*), mainly belonging to patients with succinate dehydrogenase complex, subunits *B, C,* or *D* (*SDHB, SDHC, SDHD,* collectively *SDHx*) mutations (*5–7*).

Although patients with hereditary HNPGLs are at a high risk for metastatic disease (particularly patients with *SDHB* mutations) or prone to developing multiple HNPGLs (especially those with *SDHD* mutations) (*8*), proper diagnosis of these tumors is often challenging because HNPGLs are typically biochemically silent and lack early symptoms (*4*).

Failure to accurately assess these tumors can lead to overlooked multiplicity and metastatic disease, resulting in an inappropriate follow-up, nondiagnosed heritability, and a delayed appropriate therapeutic plan with a high risk of noncurable disease.

^{18}F-fluorohydroxyphenylalanine (^{18}F-FDOPA) PET/CT, providing high sensitivity and specificity (*2,9–11*), is currently the functional imaging modality of choice in HNPGLs according to previous studies (*2,9–11*) and the current guidelines (*12,13*).

Because pheochromocytomas/paragangliomas (PPGLs) overexpress somatostatin receptors (SSTRs), especially SSTR2 (*14*), first studies were already able to show an excellent performance of ^{68}Ga-DOTA-peptides in (genetically not further evaluated) HNPGLs (*15,16*). Similar diagnostic results were shown by our group in localizing sympathetic metastatic *SDHB*-related PPGLs outside the head and neck area (*17*), which otherwise are known to have a functional imaging signature and clinical behavior significantly different from parasympathetic HNPGLs (*9,18*).

Furthermore, DOTA-peptides are used for peptide receptor radionuclide therapy (PRRT), a potentially new treatment option in patients with HNPGLs, especially those around the foramen jugulare that are rarely suitable for surgical removal (*19*). This is important, because therapeutic approaches for surgically nonremovable tumors are limited and most of these patients are not eligible for ^{131}I-metaiodobenzylguanidine (^{131}I-MIBG) treatment because of their lack of $^{123/131}$I-MIBG uptake (*9*).

Therefore, our aim was to evaluate the diagnostic utility of ^{68}Ga-DOTATATE PET/CT in *SDHB* or *SDHD* (*SDHx*)-related and other HNPGLs compared with ^{18}F-FDOPA, ^{18}F-FDG, and ^{18}F-fluorodopamine (^{18}F-FDA) PET/CT and CT/MRI, and to assess the potential eligibility of these patients for treatment with radiolabeled or cold somatostatin analogs.

MATERIALS AND METHODS

Patients

Between January 2014 and March 2015, 20 consecutive patients (11 men, 9 women) at a mean age of 48.4 ± 14.0 y were prospectively evaluated at the Eunice Kennedy Shriver National Institute of Child Health and Human Development (NICHD) of the National Institutes of Health (NIH). All patients had presented with histologically confirmed PPGL at initial diagnosis. For ethical reasons, most lesions detected on imaging studies could not be histologically confirmed in the current study. Detailed information is provided in Supplemental Table 1 (supplemental materials are available at http://jnm.snmjournals.org).

The study protocol was approved by the institutional review board of the Eunice Kennedy Shriver NICHD (protocol 00-CH-0093). All patients provided written informed consent for all clinical, genetic, biochemical, and imaging studies regarding PPGLs.

Seven patients had an *SDHD* mutation, 9 patients were positive for *SDHB*, 1 patient was positive for a hypoxia-inducible factor 2 α mutation, and 3 patients were apparently sporadic. Sixteen patients presented with additional primary PPGLs or metastatic disease (defined as PPGLs in sites in which chromaffin tissue is normally present) outside the head and neck region.

Imaging Techniques

CT scans of the neck were obtained using the following devices: Somatom Definition AS (Siemens Medical Solutions), Somatom Definition Flash (Siemens Medical Solutions), and Toshiba Aquilion ONE (Toshiba Medical Systems). Section thickness was 2 mm in the neck. All studies were performed with intravenous rapid infusion of 130 mL of nonionic water-soluble contrast agent (Isovue 300; Bracco Diagnostics), at 3–4 mL/s.

MR scans of the neck were obtained with 1.5- and 3-T scanners (Achieva 1.5 and 3 T [Philips] and Verio 1.5 T [Siemens Medical Solutions]). Image thickness was 5 mm for all neck studies. Pre- and postinjection images were obtained in the axial plane. All MR scans included axial T2 series with and without fat saturation, short tau inversion recovery series, and T1 pre- and postcontrast series after an intravenous injection of 0.2 mL/kg of body weight (Magnevist; Bayer Healthcare Pharmaceuticals).

All 20 patients underwent ^{68}Ga-DOTATATE, ^{18}F-FDOPA, and ^{18}F-FDG PET/CT as well as CT or MRI, with 18 also undergoing ^{18}F-FDA PET/CT. Fourteen patients received both a CT and an MRI of the neck whereas 3 patients received only a neck MRI and another 3 patients underwent only neck CT.

Whole-body PET/CT scans from the upper thighs to the skull were obtained 60 min after intravenous injection with mean doses of 192.4 ± 3.3 MBq of ^{68}Ga-DOTATATE, 30 min after 465.1 ± 7.4 MBq of ^{18}F-FDOPA, 60 min after 314.5 ± 81.4 MBq of ^{18}F-FDG, and approximately 8 min after 38.9 ± 0.8 MBq of ^{18}F-FDA. Sixty minutes before each ^{18}F-FDOPA scan, a dose of 200 mg of carbidopa was administered orally. All PET/CT scans were obtained on a Biograph-mCT 128 PET/CT scanner (Siemens Medical Solutions). PET imaging was obtained in 3-dimensional mode. PET images were reconstructed on a 256 × 256 matrix using an iterative algorithm provided by the manufacturer, which also uses time of flight. Low-dose CT studies for attenuation correction and anatomic coregistration were performed without contrast.

Analysis of Data

^{68}Ga-DOTATATE PET/CT studies were each interpreted independently by 2 nuclear medicine physicians, both of them with more than 10 y experience in PET and PET/CT imaging, masked to all imaging and clinical data except for the diagnosis, sex, and age of the patients. SUV_{max} was determined, and focal areas of abnormal uptake showing a higher SUV_{max} than surrounding tissue were considered as lesions. In all other imaging studies, physicians were masked to ^{68}Ga-DOTATATE PET/CT scans and clinical data except for the diagnosis, sex, and age of the patients, as well as previous imaging studies. The CT and MR images were evaluated by a neuroradiologist with over 30 y of experience in HNPGL imaging. All imaging studies were performed within 3 mo of each other. All PET/CT studies were evaluated on workstations using MedView (MedImage); CT and MRI studies were evaluated on workstations using Vue PACS (Carestream).

Histologic proof of all head and neck lesions was not feasible. Therefore, all definite head and neck foci localized with ^{18}F-FDOPA PET/CT or MRI (CT for the 3 patients in whom MRI could not be performed) were presumed to be true-positive lesions because these are the imaging modalities of choice for HNPGLs according to the current guidelines (*12,13*), with ^{18}F-FDOPA known to have excellent sensitivity and specificity (*2,9*). Because differentiation between tympanic and GJ tumors is not always feasible, these lesions were summarized as jugulotympanic (JT) tumors. Abdomen, bones, liver, lungs, and mediastinum were evaluated for metastatic disease and considered positive regardless of the number of lesions.

Statistics

For statistical analysis, the McNemar test was used to compare sensitivities between ^{68}Ga-DOTATATE PET/CT and the other imaging modalities. A 2-sided *P* value of less than 0.05 was considered significant.

TABLE 1
Lesions Identified in Head and Neck on ^{68}Ga-DOTATATE, ^{18}F-FDOPA, ^{18}F-FDG, and ^{18}F-FDA PET/CT and CT/MRI, Compared with Lesions Identified by Imaging Comparator

Lesion	^{68}Ga-DOTATATE	^{18}F-FDOPA	^{18}F-FDG	^{18}F-FDA	CT/MRI
JT	12/12	11/12	8/12	4/10	5/12
CB	10/10	10/10	9/10	0/10	8/10
GV	8/8	8/8	6/8	3/7	7/8
LN	8/8	8/8	4/8	3/7	3/8
Total	38/38	37/38	27/38	10/34	23/38

LN = lymph node.

TABLE 2
Metastatic Disease Identified in Patients and Sites Outside Head and Neck on ^{68}Ga-DOTATATE, ^{18}F-FDOPA, ^{18}F-FDG, and ^{18}F-FDA PET/CT and CT/MRI

Metastatic disease	^{68}Ga-DOTATATE	^{18}F-FDOPA	^{18}F-FDG	^{18}F-FDA	CT/MRI
Patients	16/16	13/16	13/16	6/14	15/16
Abdomen	5/5	3/5	3/5	2/4	2/5
Bones	12/12	8/12	10/12	3/11	10/12
Liver	2/2	0/2	1/2	0/2	2/2
Lungs	3/3	3/3	3/3	2/3	3/3
Mediastinum	8/8	4/8	4/8	1/7	6/8
Total sites	30/30	18/30	21/30	8/27	23/30

RESULTS

Thirty-eight lesions were identified in total on ^{18}F-FDOPA PET/CT and CT/MRI, with 37 of 38 lesions detected on ^{18}F-FDOPA PET/CT and 23 of 38 lesions detected on CT/MRI. All 38 lesions were detected on ^{68}Ga-DOTATATE PET/CT (mean SUV_{max}, 81.1 ± 83.6) as well as 7 additional head and neck lesions ($P = 0.016$) (mean SUV_{max}, 25.6 ± 27.7): 2 JT lesions, 1 GV lesion, 2 CB lesions (all related to *SDHD* mutations), and 2 lymph nodes (related to a *SDHB* mutation). Significantly fewer lesions were identified on ^{18}F-FDG PET/CT (27/38, $P < 0.01$) and ^{18}F-FDA PET/CT (10/34, $P < 0.01$). Except for the 7 lesions solely detected by ^{68}Ga-DOTATATE PET/CT, 1 JT tumor (related to an *SDHD* mutation), measuring 1.6 cm on MRI and also positive on ^{18}F-FDG and ^{68}Ga-DOTATATE, was missed on ^{18}F-FDOPA PET/CT. On CT/MRI, JT lesions and lymph nodes in particular were missed.

Detailed information about identified lesions and patient characteristics are provided in Table 1 and Supplemental Table 1.

On ^{68}Ga-DOTATATE PET/CT, metastatic disease was identified in more patients and significantly more sites ($P < 0.01$) than in all other performed scans. Detailed information is provided in Supplemental Table 1 and Table 2.

Figures 1–3 demonstrate patient examples, common sites of HNPGLs, and lesions solely detected by ^{68}Ga-DOTATATE PET/CT.

DISCUSSION

We present a comparison of ^{68}Ga-DOTATATE PET/CT to ^{18}F-FDOPA, ^{18}F-FDG, and ^{18}F-FDA PET/CT and to CT/MRI in a cohort of 20 patients with HNPGLs, 16 with underlying *SDHx*-related mutations, 1 with a hypoxia-inducible factor 2 α mutation, and 3 apparently sporadic.

On ^{68}Ga-DOTATATE PET/CT, which highly selectively binds to SSTR2, significantly more lesions were detected than with the other imaging modalities used in this study, thus confirming the utility of ^{68}Ga-DOTATATE in localizing HNPGLs and determining the possible eligibility of these patients for PRRT.

Functional imaging agents are able to target PPGLs through different mechanisms and have shown widely split performances based on tumor location and genetics.

^{18}F-FDA specifically targets catecholamine synthesis, storage, and secretion pathways and enters the cell via the norepinephrine transporter (*20*). It has shown good imaging results in the localization of primary and metastatic sympathetic but not parasympathetic PGLs (*21,22*). In this study, only 10 of 34 lesions were detected on ^{18}F-FDA PET/CT.

^{18}F-FDG is a sensitive but nonspecific radiopharmaceutical using glucose transporters (*23*). Its accumulation is related to increased glucose metabolism as seen in many different types of tumors (*23*). *SDHx*-related HNPGLs and *SDHx*-related sympathetic PGLs have shown higher glucose uptake than sporadic and other hereditary PPGLs in previous studies (*24,25*), resulting in detection rates from 77% (*9*) to 90.5% (*25*). In our study, 27 of 38 lesions were detected, resulting in a lower detection rate of 71.1%, with 16 of our 20 patients being *SDHx*-positive. One reason for this may be that JT lesions might be missed because of their proximity to the brain, which shows high glucose uptake as well, or that not only the underlying genotype but also other not-yet-discovered mechanisms might influence the glucose uptake.

^{18}F-FDOPA targets cells via the amino acid transporter system (*26*). It is the currently recommended functional imaging of choice in HNPGLs (*12,13*), proven to be sensitive and highly specific (*2,9,10*). This study confirms its strong diagnostic performance in localizing HNPGLs, identifying significantly more lesions than all other imaging modalities used except ^{68}Ga-DOTATATE PET/CT (*15*). All lesions solely visualized on ^{68}Ga-DOTATATE PET/CT were *SDHx*-positive, emphasizing a possible functional dedifferentiation of the large amino acid transporter in *SDHx* mutations.

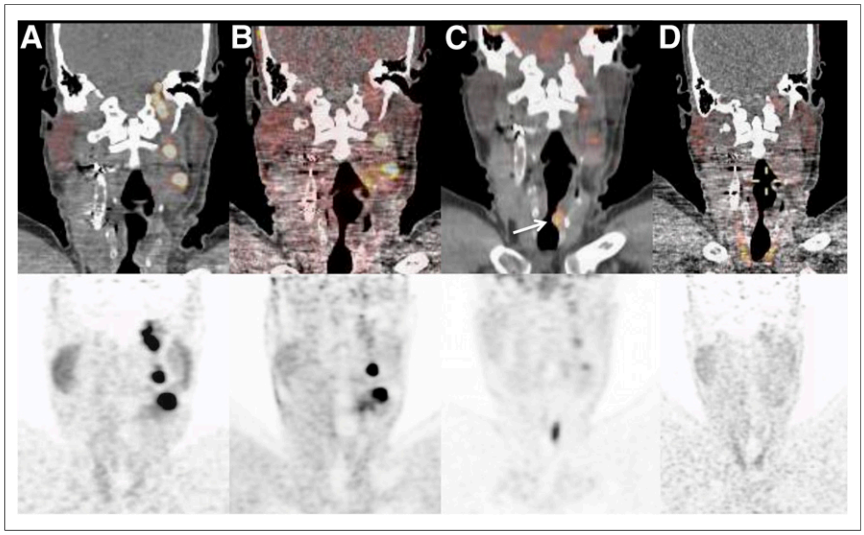

FIGURE 1. Patient 5 with *SDHD* mutation–related HNPGLs. ^{68}Ga-DOTATATE PET/CT (A) demonstrates lobulated finding in CB region on left side and additional lesion in GV region and in JT region on left side. JT findings are not visible on ^{18}F-FDOPA PET/CT (B). ^{18}F-FDG PET/CT (C) faintly demonstrates left CB and very faintly GV on left side. White arrow points to uptake in vocal cord. ^{18}F-FDA PET/CT (D) is completely negative.

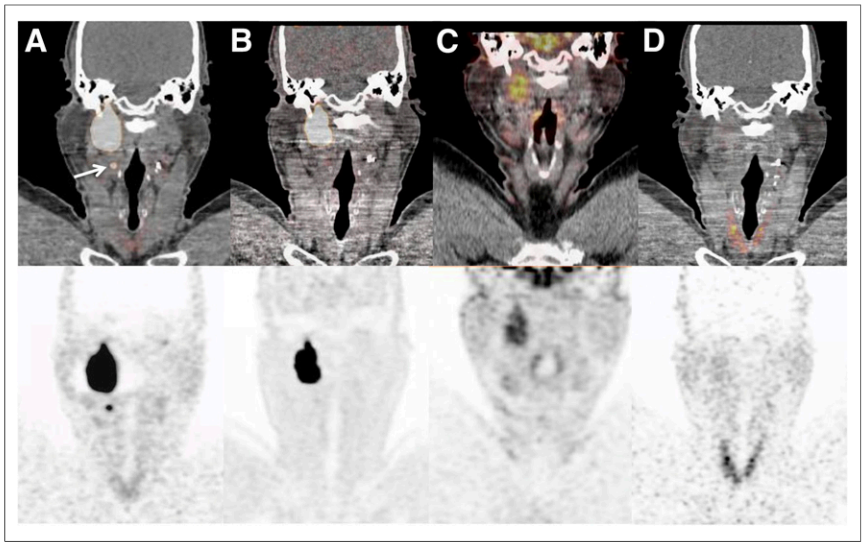

FIGURE 2. Patient 19 with *SDHD* mutation–related HNPGLs. ^{68}Ga-DOTATATE PET/CT (A) demonstrates big mass in GV region on right side and additional lesion in CB region on right (white arrow). Finding in CB region is not visible on ^{18}F-FDOPA PET/CT (B). On ^{18}F-FDG PET/CT, only GV lesion is seen faintly (C). ^{18}F-FDA PET/CT (D) is negative.

PPGLs overexpress SSTR, mainly SSTR2 (*14*). SSTR imaging with ^{111}In-DTPA-octreotide scintigraphy has already been shown to have strong diagnostic performance in parasympathetic HNPGLs (*27*). PPGL imaging with newly developed DOTA-analogs, binding to SSTR-expressing tumors much more effectively (*28*), has already been shown to have promising results (*15,16,29–31*). Recently, our group demonstrated the excellent diagnostic performance of ^{68}Ga-DOTATATE PET/CT in localizing *SDHB*-related metastatic sympathetic PPGLs (*17*), which are otherwise known to show a substantially different imaging signature in specific and unspecific functional imaging modalities (*9,18*) when compared with HNPGLs, which are of parasympathetic origin.

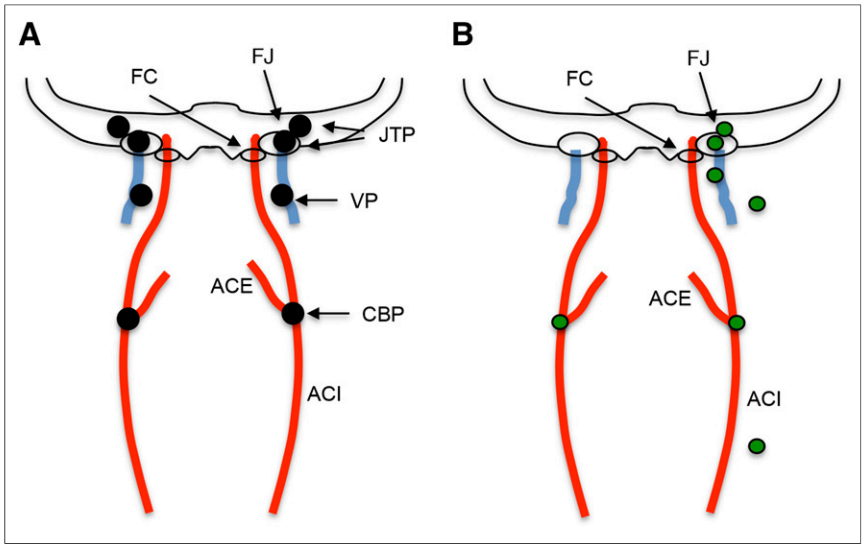

FIGURE 3. (A) Common sites of HNPGLs (black). (B) Localization of 7 lesions detected only on ^{68}Ga-DOTATATE in our study (green). ACE = external carotid artery; ACI = internal carotid artery; CBP = carotid body paraganglioma; FC = carotid foramen; FJ = jugular foramen; JTP = JT paraganglioma; VP = vagale paraganglioma.

In the current study, significantly more lesions of HNPGLs were identified on ^{68}Ga-DOTATATE PET/CT than with all other imaging modalities combined, and no additional lesions were identified on any other imaging modality. Furthermore, ^{68}Ga-DOTATATE PET/CT was able to detect metastatic disease outside the head and neck area in more patients and significantly more sites than all other imaging modalities and is therefore suggestive to have the largest impact on patient management. This finding is also in concordance with the increased expression of SSTR2A and SSTR3 found in PPGLs with an *SDH* deficiency (*32*), as most of our patients were positive for *SDHx* mutations.

Although false-positive findings cannot be fully excluded, we feel that the 7 lesions identified only by ^{68}Ga-DOTATATE PET/CT most likely represent HNPGL manifestations for the following reasons: 5 of these lesions were found in typical locations for HNPGLs, all patients had confirmed HNPGLs, and all these lesions were seen in patients with *SDHx* mutation–related disease, who are at high risk for multiple primary or metastatic lesions. Furthermore, these lesions were characterized by relatively high SUV_{max} (25.6 ± 27.7).

Besides its diagnostic value, ^{68}Ga-DOTATATE PET/CT is used to determine which patients may benefit from PRRT since surgery is not always feasible. PRRT is an established treatment option in gastroenteropancreatic NETs (*33*), and its successful use has already been reported in a limited number of patients with HNPGLs (*19,34*). Our data suggest that HNPGL patients who may benefit from PRRT could be detected with ^{68}Ga-DOTATATE PET/CT. Prospective studies will have to prove the usefulness of PRRT and the value of ^{68}Ga-DOTATATE PET/CT for the selection of these patients.

The results of the present study may also suggest that these patients can be treated with so-called cold SSTR analogs, including sandostatin LAR, lanreotide, or others. Although this has not yet been evaluated in HNPGLs, data from studies using lanreotide in gastroenteropancreatic NETs (*35*) and individual reports of octreotide treatment in patients with HNPGLs support this approach (*36,37*).

Anatomic imaging using CT/MRI is a main component of the diagnostic work-up of HNPGLs, with their greatest strength being the ability to estimate tumor delineation. However, functional imaging with ^{18}F-FDOPA and ^{68}Ga-DOTATATE PET/CT provides a higher sensitivity (*9,10,16*) and the advantage of whole-body imaging, which is especially important in the evaluation of patients with hereditary disease because of their increased risk for multiple tumors and metastases. In our study,

lesions were missed by CT/MRI especially in the JT region. This might have been avoidable by performing 3-dimensional time-of-flight or 4-dimensional MR angiographic sequences, which seem to be more sensitive in detecting HNPGLs (*2*).

Although the patients in the present study underwent many PET/CT scans, the total radiation dose of the research scans ^{68}Ga-DOTATATE, ^{18}F-FDOPA, and ^{18}F-FDA was slightly lower (~24.2 mSv) than the total expected radiation dose of the still widely used ^{123}I-MIBG and ^{111}In-DTPA-octreotide SPECT/CT (~26.1 mSv). Considering the potential of performing ^{68}Ga-DOTATATE PET/CT with even lower activities than used in our study, and considering the opportunity to combine a ^{68}Ga-DOTATATE PET/CT with a diagnostic contrast-enhanced CT in a single examination (1-stop), it might be possible to provide a desirable imaging work-up of these patients with a single imaging approach. This is supported by the fact that ^{68}Ga-DOTATATE PET/CT may be superior to other currently used functional modalities in the detection of metastatic disease (currently known mainly for *SDHx*-related PPGLs) outside the head and neck region. This imaging work-up would result in a lower radiation exposure, decreasing costs, higher patient comfort, and improved therapeutic plans.

Limitations in our study consist of its small number of patients, with a significant portion having *SDHB* mutations (although *SDHD* mutations are more common in HNPGLs), a disproportionally low number of patients with apparently sporadic tumors, the lack of patients with underlying *SDHC* mutations, and a disproportionally high number of patients with metastatic disease. Furthermore, histologic proof was not feasible for most of lesions, explicitly including those that were only positive on ^{68}Ga-DOTATATE PET/CT.

CONCLUSION

On ^{68}Ga-DOTATATE PET/CT, more lesions were identified than on all other used imaging modalities, including the current gold-standard in functional imaging, ^{18}F-FDOPA PET/CT. These results suggest a higher sensitivity and diagnostic value in the localization of *SDHx*-related and sporadic HNPGLs. Furthermore, the detection of metastatic disease outside the head and neck area was superior when using ^{68}Ga-DOTATATE PET/CT than with other imaging modalities, suggesting the possible eligibility of primary HNPGLs as well as metastatic lesions for treatment with radiolabeled or cold somatostatin analogs. As the availability and use of DOTA-analogs in imaging and therapy of various NETs increases, we predict that ^{68}Ga-DOTATATE PET/CT will become the preferred functional imaging modality for HNPGLs in the near future. However, the evaluation of the specificity of ^{68}Ga-DOTATATE in these patients is subject to further large-scale studies with extended histologic confirmation of HNPGLs.

DISCLOSURE

The costs of publication of this article were defrayed in part by the payment of page charges. Therefore, and solely to indicate this fact, this article is hereby marked "advertisement" in accordance with 18 USC section 1734. This work was supported, in part, by the Intramural Research Program of the National Institutes of Health, Eunice Kennedy Shriver National Institute of Child Health and Human Development. No other potential conflict of interest relevant to this article was reported.

REFERENCES

1. Martin TP, Irving RM, Maher ER. The genetics of paragangliomas: a review. *Clin Otolaryngol.* 2007;32:7–11.
2. Taïeb D, Kaliski A, Boedeker CC, et al. Current approaches and recent developments in the management of head and neck paragangliomas. *Endocr Rev.* 2014;35:795–819.
3. Sykes JM, Ossoff RH. Paragangliomas of the head and neck. *Otolaryngol Clin North Am.* 1986;19:755–767.
4. Erickson D, Kudva YC, Ebersold MJ, et al. Benign paragangliomas: clinical presentation and treatment outcomes in 236 patients. *J Clin Endocrinol Metab.* 2001;86:5210–5216.
5. Piccini V, Rapizzi E, Bacca A, et al. Head and neck paragangliomas: genetic spectrum and clinical variability in 79 consecutive patients. *Endocr Relat Cancer.* 2012;19:149–155.
6. Baysal BE, Willett-Brozick JE, Lawrence EC, et al. Prevalence of SDHB, SDHC, and SDHD germline mutations in clinic patients with head and neck paragangliomas. *J Med Genet.* 2002;39:178–183.
7. Neumann HP, Erlic Z, Boedeker CC, et al. Clinical predictors for germline mutations in head and neck paraganglioma patients: cost reduction strategy in genetic diagnostic process as fall-out. *Cancer Res.* 2009;69:3650–3656.
8. Neumann HP, Pawlu C, Peczkowska M, et al. Distinct clinical features of paraganglioma syndromes associated with SDHB and SDHD gene mutations. *JAMA.* 2004;292:943–951.
9. King KS, Chen CC, Alexopoulos DK, et al. Functional imaging of SDHx-related head and neck paragangliomas: comparison of ^{18}F-fluorodihydroxyphenylalanine, ^{18}F-fluorodopamine, ^{18}F-fluoro-2-deoxy-D-glucose PET, ^{123}I-metaiodobenzylguanidine scintigraphy, and ^{111}In-pentetreotide scintigraphy. *J Clin Endocrinol Metab.* 2011;96:2779–2785.
10. Hoegerle S, Ghanem N, Altehoefer C, et al. F-18-DOPA positron emission tomography for the detection of glomus tumours. *Eur J Nucl Med Mol Imaging.* 2003;30:689–694.
11. Treglia G, Cocciolillo F, de Waure C, et al. Diagnostic performance of ^{18}F-dihydroxyphenylalanine positron emission tomography in patients with paraganglioma: a meta-analysis. *Eur J Nucl Med Mol Imaging.* 2012;39:1144–1153.
12. Lenders JW, Duh QY, Eisenhofer G, et al. Pheochromocytoma and paraganglioma: an endocrine society clinical practice guideline. *J Clin Endocrinol Metab.* 2014;99:1915–1942.
13. Taïeb D, Timmers HJ, Hindie E, et al. EANM 2012 guidelines for radionuclide imaging of phaeochromocytoma and paraganglioma. *Eur J Nucl Med Mol Imaging.* 2012;39:1977–1995.
14. Reubi JC, Waser B, Schaer JC, Laissue JA. Somatostatin receptor sst1-sst5 expression in normal and neoplastic human tissues using receptor autoradiography with subtype-selective ligands. *Eur J Nucl Med.* 2001;28:836–846.
15. Kroiss A, Putzer D, Frech A, et al. A retrospective comparison between ^{68}Ga-DOTA-TOC PET/CT and ^{18}F-DOPA PET/CT in patients with extra-adrenal paraganglioma. *Eur J Nucl Med Mol Imaging.* 2013;40:1800–1808.
16. Sharma P, Thakar A, Suman KCS, et al. ^{68}Ga-DOTANOC PET/CT for baseline evaluation of patients with head and neck paraganglioma. *J Nucl Med.* 2013;54:841–847.
17. Janssen I, Blanchet EM, Adams K, et al. Superiority of [^{68}Ga]-DOTATATE PET/CT to other functional imaging modalities in the localization of SDHB-associated metastatic pheochromocytoma and paraganglioma. *Clin Cancer Res.* 2015;21:3888–3895.
18. Timmers HJ, Kozupa A, Chen CC, et al. Superiority of fluorodeoxyglucose positron emission tomography to other functional imaging techniques in the evaluation of metastatic SDHB-associated pheochromocytoma and paraganglioma. *J Clin Oncol.* 2007;25:2262–2269.
19. Puranik AD, Kulkarni HR, Singh A, Baum RP. Peptide receptor radionuclide therapy with Y/Lu-labelled peptides for inoperable head and neck paragangliomas (glomus tumours). *Eur J Nucl Med Mol Imaging.* 2015;42:1223–1230.
20. Timmers HJ, Eisenhofer G, Carrasquillo JA, et al. Use of 6-[^{18}F]-fluorodopamine positron emission tomography (PET) as first-line investigation for the diagnosis and localization of non-metastatic and metastatic phaeochromocytoma (PHEO). *Clin Endocrinol (Oxf).* 2009;71:11–17.
21. Timmers HJ, Chen CC, Carrasquillo JA, et al. Comparison of ^{18}F-fluoro-L-DOPA, ^{18}F-fluoro-deoxyglucose, and ^{18}F-fluorodopamine PET and ^{123}I-MIBG scintigraphy in the localization of pheochromocytoma and paraganglioma. *J Clin Endocrinol Metab.* 2009;94:4757–4767.
22. Ilias I, Chen CC, Carrasquillo JA, et al. Comparison of 6-^{18}F-fluorodopamine PET with ^{123}I-metaiodobenzylguanidine and ^{111}In-pentetreotide scintigraphy in localization of nonmetastatic and metastatic pheochromocytoma. *J Nucl Med.* 2008;49:1613–1619.
23. Belhocine T, Spaepen K, Dusart M, et al. ^{18}FDG PET in oncology: the best and the worst. *Int J Oncol.* 2006;28:1249–1261.

24. Timmers HJ, Chen CC, Carrasquillo JA, et al. Staging and functional characterization of pheochromocytoma and paraganglioma by ^{18}F-fluorodeoxyglucose (^{18}F-FDG) positron emission tomography. *J Natl Cancer Inst.* 2012;104:700–708.
25. Blanchet EM, Gabriel S, Martucci V, et al. ^{18}F-FDG PET/CT as a predictor of hereditary head and neck paragangliomas. *Eur J Clin Invest.* 2014;44: 325–332.
26. Havekes B, King K, Lai EW, Romijn JA, Corssmit EP, Pacak K. New imaging approaches to phaeochromocytomas and paragangliomas. *Clin Endocrinol (Oxf).* 2010;72:137–145.
27. Koopmans KP, Jager PL, Kema IP, Kerstens MN, Albers F, Dullaart RP. ^{111}In-octreotide is superior to ^{123}I-metaiodobenzylguanidine for scintigraphic detection of head and neck paragangliomas. *J Nucl Med.* 2008;49:1232–1237.
28. Reubi JC, Schar JC, Waser B, et al. Affinity profiles for human somatostatin receptor subtypes SST1-SST5 of somatostatin radiotracers selected for scintigraphic and radiotherapeutic use. *Eur J Nucl Med.* 2000;27:273–282.
29. Maurice JB, Troke R, Win Z, et al. A comparison of the performance of ^{68}Ga-DOTATATE PET/CT and ^{123}I-MIBG SPECT in the diagnosis and follow-up of phaeochromocytoma and paraganglioma. *Eur J Nucl Med Mol Imaging.* 2012;39:1266–1270.
30. Naji M. A AL-N. ^{68}Ga-labelled peptides in the management of neuroectodermal tumours. *Eur J Nucl Med Mol Imaging.* 2012;39(suppl 1):S61–S67.
31. Naji M, Zhao C, Welsh SJ, et al. ^{68}Ga-DOTA-TATE PET vs. ^{123}I-MIBG in identifying malignant neural crest tumours. *Mol Imaging Biol.* 2011;13: 769–775.
32. Elston MS, Meyer-Rochow GY, Conaglen HM, et al. Increased SSTR2A and SSTR3 expression in succinate dehydrogenase-deficient pheochromocytomas and paragangliomas. *Hum Pathol.* 2015;46:390–396.
33. Kwekkeboom DJ, de Herder WW, Kam BL, et al. Treatment with the radiolabeled somatostatin analog [177 Lu-DOTA 0,Tyr3]octreotate: toxicity, efficacy, and survival. *J Clin Oncol.* 2008;26:2124–2130.
34. Zovato S, Kumanova A, Dematte S, et al. Peptide receptor radionuclide therapy (PRRT) with ^{177}Lu-DOTATATE in individuals with neck or mediastinal paraganglioma (PGL). *Horm Metab Res.* 2012;44:411–414.
35. Caplin ME, Pavel M, Cwikla JB, et al. Lanreotide in metastatic enteropancreatic neuroendocrine tumors. *N Engl J Med.* 2014;371:224–233.
36. Elshafie O, Al Badaai Y, Alwahaibi K, et al. Catecholamine-secreting carotid body paraganglioma: successful preoperative control of hypertension and clinical symptoms using high-dose long-acting octreotide. *Endocrinol Diabetes Metab Case Rep.* 2014;2014:140051.
37. Kau R, Arnold W. Somatostatin receptor scintigraphy and therapy of neuroendocrine (APUD) tumors of the head and neck. *Acta Otolaryngol.* 1996;116: 345–349.